

Quantum forking for fast weighted power summation

Daniel K. Park,^{1,2,*} Ilya Sinayskiy,^{3,4,†} Mark Fingerhuth,^{3,5,‡}

Francesco Petruccione,^{3,4,§} and June-Koo Kevin Rhee^{1,2,3,¶}

¹*School of Electrical Engineering, KAIST, Daejeon, 34141, Republic of Korea*

²*ITRC of Quantum Computing for AI,*

KAIST, Daejeon, 34141, Republic of Korea

³*Quantum Research Group, School of Chemistry and Physics,*

University of KwaZulu-Natal, Durban,

KwaZulu-Natal, 4001, South Africa

⁴*National Institute for Theoretical Physics (NITheP),*

KwaZulu-Natal, 4001, South Africa

⁵*ProteinQure Inc., Toronto, M5T 2C2, Canada*

Abstract

The computational cost of preparing an input quantum state can be significant depending on the structure of data to be encoded. Many quantum algorithms require repeated sampling to find the answer, mandating reconstruction of the same input state for every execution of an algorithm. Thus, the advantage of quantum information processing can diminish due to redundant state initialization. Here we present a framework based on quantum forking that bypasses such a fundamental issue and expedites a weighted power summation of measurement outcomes from independent quantum processes. Our approach uses quantum interference to add up expectation values measured from independent quantum trajectories created in superposition by quantum forking, while requiring only a single initial state preparation routine. As examples, we describe applications of the framework for entanglement witnesses and purity benchmarking. A proof-of-principle experiment is implemented on the IBM and Rigetti quantum cloud platforms.

* kpark10@kaist.ac.kr

† sinayskiy@ukzn.ac.za

‡ markfingerhuth@gmail.com

§ petruccione@ukzn.ac.za

¶ rhee.jk@kaist.edu

I. INTRODUCTION

Designing an efficient quantum algorithm to solve a computational task does not alone ensure a quantum advantage over a classical counterpart, but there must also be an efficient procedure to prepare the desired initial quantum state. Existing methods for preparing an arbitrary quantum state [1–9], a famous example being quantum random access memory (QRAM) [10–14], introduce resource overheads, even though the hardware and process complexities may scale efficiently with respect to the size of the data to be encoded. It is therefore imperative to minimize the number of state preparation routines. However, an input quantum state prepared for a specific algorithm cannot be reused for another task once measured due to the measurement postulate of quantum mechanics. Moreover, the quantum state cannot be cloned. Hence, in general, one is forced to generate an input state in every execution of a quantum algorithm. However, many quantum information processing (QIP) tasks rely on repeating the measurement for sampling the answer. Thus the true advantage of harnessing quantum mechanics for information processing becomes unclear when the aforementioned redundancy is imposed. As a means to circumvent this fundamental issue in certain applications, quantum forking (QF) was introduced in Ref. [14], motivated by forking in classical operating systems that creates a separate address space for a child process for multitasking [15]. In Ref. [14], the application was limited to estimating the inner product of quantum states.

In this work, we develop quantum forking-based weighted power summation (QFS) to accelerate various tasks for which one needs to implement independent propagation of the quantum trajectories and eventually sum the measurement outcomes. With this approach, the number of state preparation routines necessary for estimating a weighted power sum of measurement outcomes sampled from any number of independent quantum processes remains constant, though this is at the cost of introducing a control qudit, ancilla qubits in arbitrary states, and a series of controlled swap gates. Moreover, QFS can be used to effectively measure an arbitrary observable using the ability to sum independent measurement results efficiently. This is particularly useful when directly measurable observables are limited by experimental constraints. We use entanglement witness and purity benchmarking as example applications to demonstrate the relevance and utility of QFS to quantum information science. We also realize a proof-of-principle experiment of a QFS on two quantum

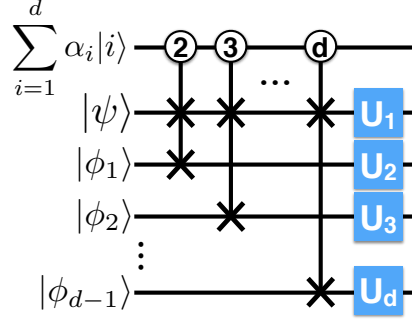


FIG. 1. Quantum forking circuit to create d independent processes in superposition. The numbers in circles indicate the qudit state that activates the controlled swap gate.

computers in the cloud, the IBM Q 5 Tenerife [16] and Rigetti 16Q Aspen-1 [17].

Furthermore, when large-scale quantum hardware becomes available, a quantum operating system that deploys efficient resource management and acts as an interface between qubits and quantum programs is of fundamental importance [18]. Along with QRAM, the quantum forking algorithm developed here has the potential to be used as a building block for such a quantum operating system.

II. QUANTUM FORKING

Quantum forking is a process that creates an entangled state to allow a target quantum state $|\psi\rangle$ to undergo d independent evolutions in superposition [14]. At the end of the computation, some measurement procedure is employed to find the desired answer more efficiently compared to when the quantum state undergoes these evolutions one at a time. This can be achieved by coupling the target state $|\psi\rangle$ to a control qudit (or $\log_2(d)$ qubits) and $d - 1$ ancilla qubits in some arbitrary state $|\phi_j\rangle$, such that the target state undergoes independent processes in d orthogonal subspaces. The quantum circuit for realizing QF is depicted in Fig. 1. The quantum forking is initiated by the series of controlled swap (c-swap)

gates controlled by the state of the qudit. These gates evolve the total state as

$$\begin{aligned}
|\Psi\rangle &= \alpha_1 |1\rangle \otimes |\psi\rangle \otimes |\phi_1\rangle \otimes |\phi_2\rangle \otimes \dots \otimes |\phi_{d-1}\rangle \\
&+ \alpha_2 |2\rangle \otimes |\phi_1\rangle \otimes |\psi\rangle \otimes |\phi_2\rangle \otimes \dots \otimes |\phi_{d-1}\rangle \\
&+ \dots \\
&+ \alpha_d |d\rangle \otimes |\phi_{d-1}\rangle \otimes |\phi_1\rangle \otimes |\phi_2\rangle \otimes \dots \otimes |\psi\rangle.
\end{aligned} \tag{1}$$

Hereinafter, the tensor product symbol is omitted for brevity when the meaning is clear. The above expression shows that QF creates an entangled state whereby the target quantum state $|\psi\rangle$ is encoded in a different qubit for each subspace referenced by the control qudit. Thus, by applying local unitaries, the target quantum state can undergo d independent processes simultaneously. For instance, the total state after the application of local unitary operators becomes

$$\begin{aligned}
|\Psi\rangle &= \alpha_1 |1\rangle U_1 |\psi\rangle U_2 |\phi_1\rangle U_3 |\phi_2\rangle \dots U_d |\phi_{d-1}\rangle \\
&+ \alpha_2 |2\rangle U_1 |\phi_1\rangle U_2 |\psi\rangle U_3 |\phi_2\rangle \dots U_d |\phi_{d-1}\rangle \\
&+ \dots \\
&+ \alpha_d |d\rangle U_1 |\phi_{d-1}\rangle U_2 |\phi_1\rangle U_3 |\phi_2\rangle \dots U_d |\psi\rangle.
\end{aligned} \tag{2}$$

The ancilla qubits can be untouched if desired, by controlling the unitary operators with the qudit state.

III. QUANTUM FORKING FOR WEIGHTED POWER SUMMATION

Quantum forking can be furnished with a measurement procedure to evaluate a weighted power sum of the following form with only a constant number of initial state generations:

$$\sum_{i=1}^d p_i \prod_{j=1}^q \langle M_{i,j} \rangle, \tag{3}$$

where p_i is a non-negative real number satisfying $\sum p_i = 1$, q is a positive integer, and $M_{i,j}$ is an observable. In general, estimating Eq. (3) to within ϵ with a probability of error δ requires $O(q'd \log(1/\delta)/\epsilon^2)$ state preparations [19], where $q' \leq q$ is the number of unique observables in the non-linear sum. QFS yields the same result with $O(q \log(1/\delta)/\epsilon^2)$ state preparations, reducing the time complexity by about a factor of d . In the following, we explain QFS for

linear ($q = 1$) and quadratic ($q = 2$) sums using the cases where $M_{i,1} = M_{i,2}$ and $d = 2$. In these cases, QFS reduces the number of initial state generation routines by a factor of two.

Adding two expectation value measurement outcomes with equal weights can be done with one control qubit and one ancilla qubit in an arbitrary state $|\phi\rangle$, as depicted in Fig. 2(a). First, the control qubit is prepared in the equal superposition state via the Hadamard gate (denoted H). The first c-swap gate then yields

$$|\Phi_1\rangle = \frac{|0\rangle|\psi\rangle|\phi\rangle + |1\rangle|\phi\rangle|\psi\rangle}{\sqrt{2}}. \quad (4)$$

The two local unitaries transform the above state to

$$|\Phi_2\rangle = \frac{|0\rangle U_1|\psi\rangle U_2|\phi\rangle + |1\rangle U_1|\phi\rangle U_2|\psi\rangle}{\sqrt{2}}. \quad (5)$$

Finally, another c-swap gate *unforks*, i.e., reverses the forking, such that the final state is

$$|\Phi_f\rangle = \frac{|0\rangle U_1|\psi\rangle U_2|\phi\rangle + |1\rangle U_2|\psi\rangle U_1|\phi\rangle}{\sqrt{2}}. \quad (6)$$

Now the expectation value of an observable M measured on the target qubit gives the desired average of the two quantities:

$$\begin{aligned} \langle M \rangle &= \langle \Phi_f | \mathbb{1} \otimes M \otimes \mathbb{1} | \Phi_f \rangle \\ &= \frac{1}{2} (\langle 0|0\rangle \langle M_1 \rangle \langle \phi | U_2^\dagger U_2 | \phi \rangle + \langle 1|1\rangle \langle M_2 \rangle \langle \phi | U_1^\dagger U_1 | \phi \rangle) \\ &= \frac{1}{2} (\langle M_1 \rangle + \langle M_2 \rangle), \end{aligned} \quad (7)$$

where $M_j = U_j^\dagger M U_j$.

If one performs the local measurement on both target and ancilla qubits without unforking, i.e., directly on $|\Phi_2\rangle$, the measurement outcomes are $\langle \Phi_2 | \mathbb{1} \otimes M \otimes \mathbb{1} | \Phi_2 \rangle = (\langle \psi | M_1 | \psi \rangle + \langle \phi | M_1 | \phi \rangle)/2$ and $\langle \Phi_2 | \mathbb{1} \otimes \mathbb{1} \otimes M | \Phi_2 \rangle = (\langle \psi | M_2 | \psi \rangle + \langle \phi | M_2 | \phi \rangle)/2$. Thus if $\langle \phi | M_j | \phi \rangle$ is known, the linear sum shown in Eq. (7) can be calculated without the reversal c-swap gate at the cost of performing the local measurement on the ancilla qubit as well. We narrow our discussion to the general case without such *a priori* information, and focus on the quantum forking with the unforking step.

There are several interesting remarks. First, the ancilla state $|\phi\rangle$ can be arbitrary and even unknown. As a result, one can use any state that is the easiest to prepare in the given experimental setup, such as a thermal equilibrium state or a leftover state from the

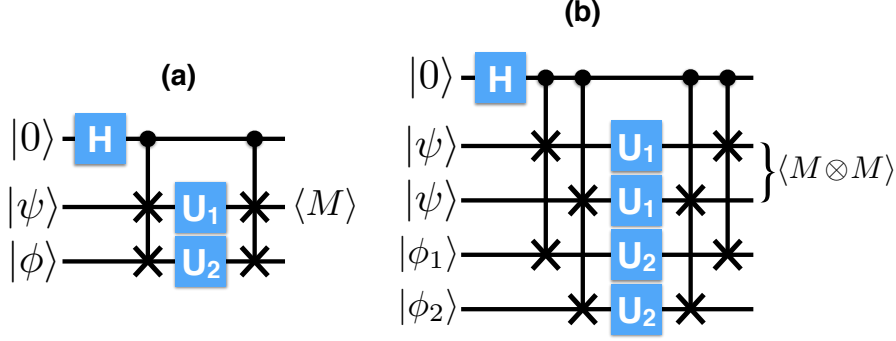


FIG. 2. Quantum forking-based circuits for evaluating (a) linear and (b) quadratic sums of two expectation values.

previous algorithm. We assume that the computational cost of preparing such states is negligible compared to the cost of $|\psi\rangle$ preparation. Second, one can easily verify that the same outcome can be obtained when the control qubit is initially prepared in $|1\rangle$, since this only alters the sign of the second term in Eq. (4), which cannot be detected in the expectation value measurement. Thus the maximally mixed state can be used as the initial state of the control qubit. This state is more difficult to prepare compared to an arbitrary state $|\phi\rangle$, but we assume that the cost is still negligible compared to that of the preparation of $|\psi\rangle$. Third, the weights p_i can be manipulated by initializing the control state to either a mixed state $\sum_i p_i |i\rangle\langle i|$, or a pure state $\sum_i \sqrt{p_i} |i\rangle$. Finally, the unitary operators can be replaced with any quantum channel. The last two remarks are supported by the following. Let the initial state be represented as a density matrix $\rho_i = (p_1|0\rangle\langle 0| + p_0|1\rangle\langle 1|) \otimes \rho_\psi \otimes \rho_\phi$. The full QFS protocol produces the final density matrix $\rho_f = p_1|0\rangle\langle 0| \otimes \Lambda_1(\rho_\psi) \otimes \Lambda_2(\rho_\phi) + p_2|1\rangle\langle 1| \otimes \Lambda_2(\rho_\psi) \otimes \Lambda_1(\rho_\phi)$, where Λ_j is a completely positive trace preserving (CPTP) map. Then the expectation value measurement gives

$$\begin{aligned}
 \langle M \rangle &= \text{tr}(\mathbb{1} \otimes M \otimes \mathbb{1} \rho_f) \\
 &= p_1 \text{tr}(|0\rangle\langle 0|) \text{tr}(M \Lambda_1(\rho_\psi)) \text{tr}(\Lambda_2(\rho_\phi)) + p_2 \text{tr}(|1\rangle\langle 1|) \text{tr}(M \Lambda_2(\rho_\psi)) \text{tr}(\Lambda_1(\rho_\phi)) \\
 &= p_1 \text{tr}(M \Lambda_1(\rho_\psi)) + p_2 \text{tr}(M \Lambda_2(\rho_\psi)).
 \end{aligned} \tag{8}$$

Since off-diagonal terms in the density matrix of the control qubit vanish in the expectation value evaluation, the result provided in Eq. (8) also holds for a control qubit initialized in a pure state with probability amplitudes whose absolute squares correspond to the weights.

To evaluate the squared sum of expectation values with QFS, two qubits prepared in $|\psi\rangle$

and two arbitrary (even unknown) ancillae are required. A series of **c-swap** gates initiates QF, and each pair of the qubits experiences the independent unitary evolutions denoted by U_1 and U_2 , respectively. After additional **c-swap** gates unfork, the final state is given as

$$|\Psi_f\rangle = \frac{1}{\sqrt{2}}(|0\rangle U_1|\psi\rangle U_1|\psi\rangle U_2|\phi_1\rangle U_2|\phi_2\rangle + |1\rangle U_2|\psi\rangle U_2|\psi\rangle U_1|\phi_1\rangle U_1|\phi_2\rangle). \quad (9)$$

Now measuring $\langle M \otimes M \rangle$ on the target qubits gives

$$\begin{aligned} \langle M \otimes M \rangle &= \langle \Psi_f | \mathbb{1} \otimes M \otimes M \otimes \mathbb{1} \otimes \mathbb{1} | \Psi_f \rangle \\ &= \frac{1}{2} (\langle 0|0\rangle \langle \psi | M_1 | \psi \rangle \langle \psi | M_1 | \psi \rangle \langle \phi_1 | U_2^\dagger U_2 | \phi_1 \rangle \langle \phi_2 | U_2^\dagger U_2 | \phi_2 \rangle \\ &\quad + \langle 1|1\rangle \langle \psi | M_2 | \psi \rangle \langle \psi | M_2 | \psi \rangle \langle \phi_1 | U_1^\dagger U_1 | \phi_1 \rangle \langle \phi_2 | U_1^\dagger U_1 | \phi_2 \rangle) \\ &= \frac{1}{2} (\langle M_1 \rangle^2 + \langle M_2 \rangle^2). \end{aligned} \quad (10)$$

The procedure is shown in Fig. 2(b). By the same argument used above, the maximally mixed state can be used as the initial state of the control qubit, and any local CPTP map can be used instead of the local unitaries. Moreover, the control qubit can be replaced with a mixed state $\sum_i p_i |i\rangle\langle i|$, or a pure state $\sum_i \sqrt{p_i} |i\rangle$ in order to assign unequal weights. Note that more general non-linear sums, such as $\sum_i^d p_i \langle M_i \rangle \langle N_i \rangle$, can also be evaluated by measuring $\langle M \otimes N \rangle$.

To evaluate the most general case of Eq. (3) with QF, one needs to perform $O(\log(1/\delta)/\epsilon^2)$ quantum forking experiments with q target qubits, 1 control qudit of dimension d , $q(d-1)$ ancilla qubits in any arbitrary (even unknown) states, and $2q(d-1)$ **c-swap** gates. The control qudit can be in the mixed state where an i th diagonal element of the density matrix dictates the weight p_i . For uniform weights, i.e., $p_i = 1/\sqrt{d} \forall i$, the control qudit can be in the maximally mixed state. The advantage of QFS becomes apparent when d is large and the preparation of the initial target state $|\psi\rangle$ is complex. The temporal cost of repeating the individual quantum circuits is traded for the spatial cost of having the ancilla qubits in QF. But these ancilla qubits can be in any arbitrary state, and hence the cost of preparing them is negligible. In fact, the same ancilla qubit can be repeatedly used for multiple QFS tasks without having to be reinitialized. Another notable aspect is that the dephasing error on the control qubit does not alter the result since only the diagonal terms in the density matrix of the control qubit contributes to the expectation value evaluation. On the other hand, QFS may be impractical for large q when the q -local measurement is experimentally challenging to perform.

IV. APPLICATIONS

QFS for linear and quadratic summations can be valuable in various QIP tasks as we now demonstrate with the following examples.

The linear summation can be utilized in the experimental measurement of entanglement witnesses (EW). An EW is an observable that distinguishes an entangled state from separable ones, and is generally a useful tool in quantum information science for studying entanglement without relying on expensive quantum state tomography [20]. More formally, the expectation measurement of an entanglement witness W gives $\text{tr}(W\rho_{sep}) \geq 0$ for all separable state ρ_{sep} , while there exists an entangled state ρ_{ent} such that $\text{tr}(W\rho_{ent}) < 0$. An EW can also be viewed as a hyperplane separating some entangled states from the set of separable states [21]. Since W is a Hermitian operator, it can be written as a weighted sum of other Hermitian operators, i.e., $W = \sum_i c_i A_i$, $A_i = A_i^\dagger \forall i$, and $c_i \in \mathbb{R} \forall i$. Thus, an EW can be constructed by measuring the expectation values of experimentally available observables A_i , and post-processing the measurement outcomes with appropriate weights. With this, the benefit of QF becomes apparent; instead of measuring the observables needed to construct the linear sum individually, QFS yields the same result by measuring the expectation value of a single observable, i.e., the one that is the easiest to measure in the laboratory, such as σ_z . To elucidate such a QFS application, we can consider an EW which determines whether a given state is useful for performing quantum teleportation via QFS. The teleportation witness operator can be written as $W_t = (\mathbb{1} \otimes \mathbb{1} - \sigma_x \otimes \sigma_x + \sigma_y \otimes \sigma_y - \sigma_z \otimes \sigma_z) / 4$ in terms of Pauli operators [22]. A naive witness experiment requires measuring three two-qubit Pauli observables. Alternatively, the same quantity can be evaluated with the QFS circuit shown in Fig. 3. Since there are three independent observables to be measured, i.e., $d = 3$, a qutrit is needed to create three forking trajectories. Without loss of generality, the ancilla qubits are all in the same state $|\phi\rangle$ in the figure, but they can be in any state without altering the final outcome. Using $H\sigma_z H = \sigma_x$, $S\sigma_x S^\dagger = -S^\dagger\sigma_x S = \sigma_y$, where S denotes the phase gate, it is straightforward to verify that the measurement of $\langle \sigma_z \otimes \sigma_z \rangle$ on the target two-qubit state yields $\langle \sigma_x \otimes \sigma_x - \sigma_y \otimes \sigma_y + \sigma_z \otimes \sigma_z \rangle$. From this, W_t can be obtained. Therefore, the use of QF reduces the number of Pauli observables to be measured from three to one. In practice, qutrits may not be available in a given experimental setup, and it could be easier to prepare qubits. In the next example, we explain how to create three independent processes

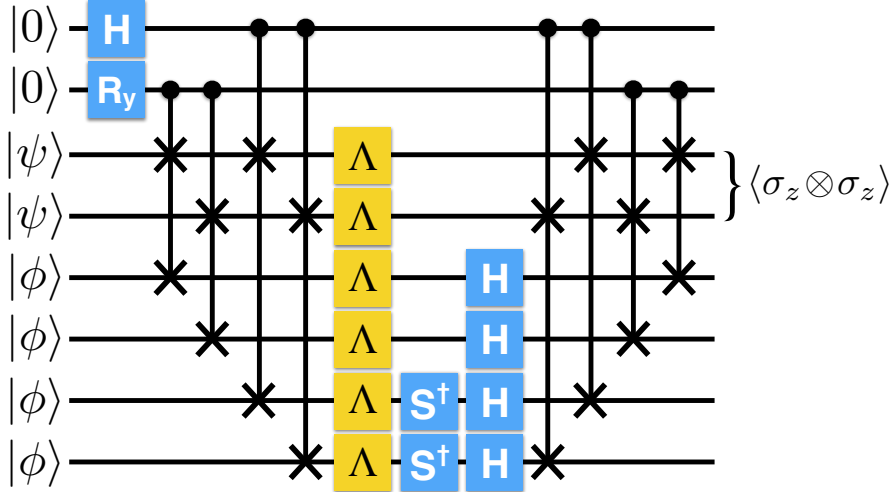


FIG. 4. Quantum forking-based circuit for calculating the purity of a single qubit after being transmitted through a quantum channel Λ .

forkings can occur with the control states $|00\rangle$, $|10\rangle$, and $(|01\rangle + |11\rangle)/\sqrt{2}$, allowing the given trajectories to be measured with equal probabilities as desired. The QF circuit for the single qubit purity measurement is depicted in Fig. 4. As before, the ancilla qubits are all in the same state $|\phi\rangle$, but any state can be used without altering the final outcome. The target qubits and the ancillae first undergo the same single-qubit quantum channel Λ . But just before unforking, either H or HS^\dagger are applied to measure $H\sigma_zH = \sigma_x$ or $SH\sigma_zHS^\dagger = \sigma_y$, as desired in the purity measurement.

V. EXPERIMENTS

We present the experimental results from a proof-of-principle implementation of QFS using the IBM Q 5 Tenerife [16] and Rigetti 16Q Aspen-1 [17] quantum processors. Suppose a single qubit is prepared by rotating $|0\rangle$ around an unknown axis, either x, y or z, of the Bloch sphere by a known angle θ . After the state preparation, by measuring at least two Pauli observables, the axis of rotation can be discriminated. Alternatively, the sum of any two Pauli expectation values can be used. For example, $\langle\sigma_z + \sigma_x\rangle$ results in $\cos(\theta)$, $\cos(\theta) + \sin(\theta)$ or 1 for the rotation along x, y or z axis, respectively. Thus by measuring $\langle\sigma_z + \sigma_x\rangle$ with respect to θ reveals the rotating axis. A simple three-qubit QFS with one Pauli expectation measurement can evaluate the same quantity. The QFS circuit implemented with IBM and

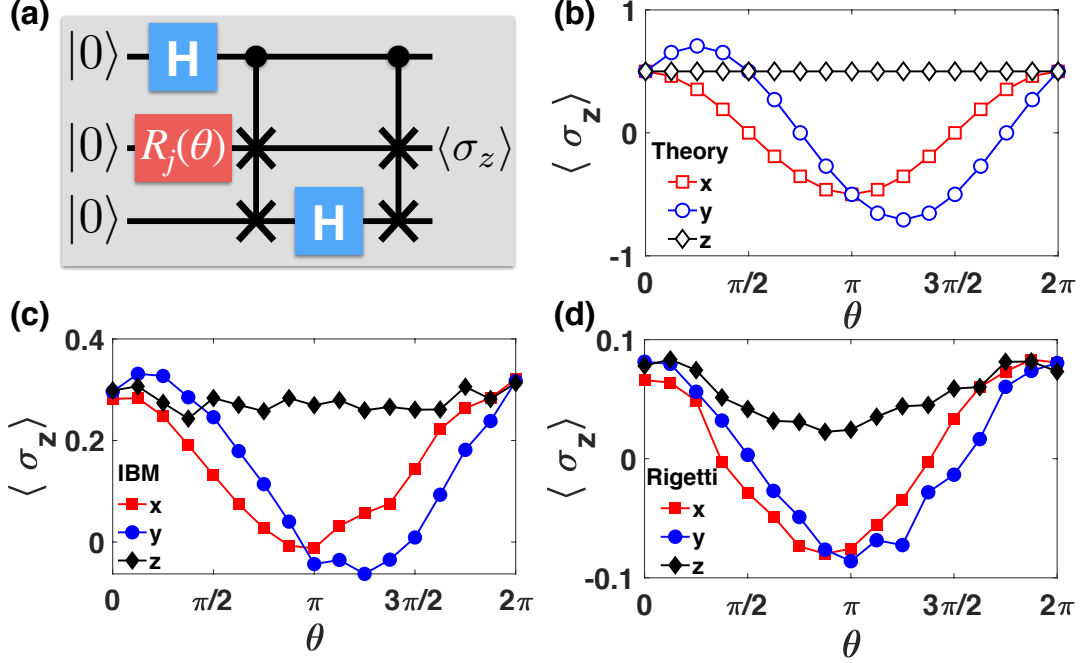


FIG. 5. (a) Quantum forking-based circuit for discriminating the axis of the single qubit rotation in the Bloch sphere. $R_j(\theta)$ represents the single qubit rotation around j by θ . Results from theory, IBM Q 5 Tenerife and Rigetti 16Q Aspen-1 are shown in (b), (c), and (d), respectively. Square, circle and diamond are for $j = x, y$ and z , respectively.

Rigetti cloud quantum computers is shown in Fig. 5(a). After creating two forking paths via the first c-**swap** gate, a Hadamard operation is applied to the ancilla qubit for the $\langle \sigma_x \rangle$ measurement. Then the final c-**swap** gate is applied to unfork, and $\langle \sigma_z \rangle$ measurement on the target qubit yields the desired outcome. Theoretical calculations and experimental data obtained using the IBM and Rigetti quantum processors are compared in Fig. 5(b), (c) and (d). The square, circle and diamond symbols represent the expectation value of σ_z when the rotation of an angle θ is applied along the x, y and z axis, respectively. For each axis, three sets of experiments are performed with a different direction of changing θ , that is varied from 0 to 2π in increments of $\pi/8$, and the results are averaged in order to suppress experimental bias in the direction of θ that may arise due to drift in calibration. In the first and second sets, θ is uniformly increased and uniformly decreased, respectively. In the last set, θ is randomly selected between 0 and 2π in $\pi/8$ increments. Each experiment is repeated for 8192 runs to collect measurement statistics. Thus each data shown in Fig. 5(c) and (d) is an average of 24576 runs. Despite experimental deviations from theory as illustrated with

the amplitudes errors of the curves, the QFS protocol manifests successful discrimination of the initially unknown axis of the rotation with only a single expectation value measurement using currently available cloud quantum computers.

VI. CONCLUSION

In summary, we have presented quantum forking as a tool to reduce the time complexity of general weighted power summation. Quantum forking encodes quantum information in different subspaces of an entangled state. Then each subspace undergoes independent quantum trajectories. With this technique, the q th power summation of d measurement outcomes with arbitrary weights can be carried out with the constant cost of initial state preparation, while requiring $q(d - 1)$ ancilla qubits given in arbitrary states, a control qudit with dimension d , q -local measurement and $2q(d - 1)$ c-swap gates. The number of state preparation routines is reduced by $O(d)$, and hence QFS is particularly useful when d is large, the state preparation procedure is complex, and q is relatively small, i.e., less than three or so. We also showed how QF can be utilized in entanglement witnesses and purity benchmarking. Finally, we demonstrated the proof-of-principle using the cloud quantum computers from IBM and Rigetti. In future work, we plan to apply QFS for quantum Monte Carlo simulations, such as those used for quantum master equation unravelling [25], where the solutions of the quantum master equation can be obtained as an ensemble average of the solutions to the stochastic Schrödinger equation.

ACKNOWLEDGMENTS

We acknowledge use of IBM Q and Rigetti Quantum Cloud Services for this work. The views expressed are those of the authors and do not reflect the official policy or position of IBM or the IBM Q team. The use of Rigetti hardware was made possible through the Developer Partnership between Rigetti and ProteinQure. We thank the Rigetti team for help associated with the Quantum Cloud Services. This work was supported in parts by the Ministry of Science and ICT, Korea, under an ITRC Program, IITP-2018-2018-0-01402, and an NRF Program, 2018K1A3A1A09078001, and by the South African Research Chair Initiative of the Department of Science and Technology and the National Research

Foundation. We thank Dr. Graeme Pleasance for proofreading the manuscript.

- [1] L. M. Sieberer and W. Lechner, *Phys. Rev. A* **97**, 052329 (2018).
- [2] G.-L. Long and Y. Sun, *Phys. Rev. A* **64**, 014303 (2001).
- [3] A. N. Soklakov and R. Schack, *Phys. Rev. A* **73**, 012307 (2006).
- [4] M. Mosca and P. Kaye, in *Optical Fiber Communication Conference and International Conference on Quantum Information* (Optical Society of America, 2001) p. PB28.
- [5] L. Grover and T. Rudolph, arXiv:quant-ph/0208112 [quant-ph] (2002).
- [6] M. Plesch and Č. Brukner, *Phys. Rev. A* **83**, 032302 (2011).
- [7] J. J. Vartiainen, M. Möttönen, and M. M. Salomaa, *Phys. Rev. Lett.* **92**, 177902 (2004).
- [8] D. Ventura and T. Martinez, *Information Sciences* **124**, 273 (2000).
- [9] M. Möttönen, J. J. Vartiainen, V. Bergholm, and M. M. Salomaa, *Quantum Info. Comput.* **5**, 467 (2005).
- [10] V. Giovannetti, S. Lloyd, and L. Maccone, *Phys. Rev. Lett.* **100**, 160501 (2008).
- [11] V. Giovannetti, S. Lloyd, and L. Maccone, *Phys. Rev. A* **78**, 052310 (2008).
- [12] F.-Y. Hong, Y. Xiang, Z.-Y. Zhu, L.-z. Jiang, and L.-n. Wu, *Phys. Rev. A* **86**, 010306 (2012).
- [13] S. Arunachalam, V. Gheorghiu, T. Jochym-OConnor, M. Mosca, and P. V. Srinivasan, *New Journal of Physics* **17**, 123010 (2015).
- [14] D. K. Park, F. Petruccione, and J.-K. K. Rhee, arXiv:1901.02362 [quant-ph] (2019; also to be published in Scientific Report).
- [15] D. M. Ritchie and K. Thompson, *Commun. ACM* **17**, 365 (1974).
- [16] 5-qubit backend: IBM Q team, "IBM Q 5 Tenerife backend specification v1.3.0," (2018). <https://ibm.biz/qiskit-tenerife>, Last Accessed: 2018-11.
- [17] Rigetti computing, 16Q Aspen-1, <https://www.rigetti.com/qpu>, Last Accessed: 2019-02.
- [18] H. Corrigan-Gibbs, D. J. Wu, and D. Boneh, in *Proceedings of the 16th Workshop on Hot Topics in Operating Systems, HotOS '17* (ACM, New York, NY, USA, 2017) pp. 76–81.
- [19] P. J. Huber, *Robust Statistics* (Wiley, New York, 1981).
- [20] D. Chruściński and G. Sarbicki, *Journal of Physics A: Mathematical and Theoretical* **47**, 483001 (2014).
- [21] B. M. Terhal, *Physics Letters A* **271**, 319 (2000).

- [22] N. Ganguly, S. Adhikari, A. S. Majumdar, and J. Chatterjee, *Phys. Rev. Lett.* **107**, 270501 (2011).
- [23] J. Wallman, C. Granade, R. Harper, and S. T. Flammia, *New Journal of Physics* **17**, 113020 (2015).
- [24] G. Feng, J. J. Wallman, B. Buonacorsi, F. H. Cho, D. K. Park, T. Xin, D. Lu, J. Baugh, and R. Laflamme, *Phys. Rev. Lett.* **117**, 260501 (2016).
- [25] H. P. Breuer and F. Petruccione, *The Theory of Open Quantum Systems* (Oxford University Press, 2007).